CHAPTER 4

LIGHT EXTINCTION AND ITS RELATIONSHIP TO AEROSOLS

In this chapter the relationship between aerosol concentration and measured extinction will be explored. Transmissometers are operated at a number of sites, in part, as a quality assurance check on apportionment of extinction to aerosol species. It is anticipated that the estimated scattering and absorption associated with the various aerosol species should sum to equal the measured extinction. However, White [1990] and Trijonis [1990] have shown that under some conditions this assumption may not be true. One difficulty in reconstructing extinction is the accurate estimation of absorption. The IMPROVE data set, along with the Measurements of Haze and Visual Effects (MOHAVE) special study data set, allow for a unique opportunity to explore the interrelationships between aerosol mass and absorption. From these intercomparisons a "best estimate" of scattering and absorption efficiencies will be developed for purposes of calculating the contribution of each aerosol species to extinction and therefore visibility impairment.

In 1991, Congress mandated a regional haze study whose goal was to assess the contribution of the Mohave Power Project (MPP), other nearby point sources, and regional emissions to visibility impairment in Grand Canyon National Park. The location of monitoring sites, selected national parks and wilderness areas, and major urban areas, are shown in Figure 4.1. The MOHAVE study was carried out over a period of one year (1992) with two major field intensives during the summer and winter months. An objective of MOHAVE was to apportion (or attribute) the haze observed in the Grand Canyon region to the various measured aerosol species. One set of measurements made during the summer intensive at Meadview, Lake Mead National Recreation Area, employed independent measurements of b_{ext}, b_{scat}, and b_{abs} using optical techniques as well as a full suite of aerosol mass concentrations including carbonaceous material. Independent measurements of these three variables allow for internal consistency checks on the optical measurements in that absorption and scattering should sum to extinction. Furthermore, the sum of aerosol scattering should equal measured scattering, and absorption estimated from measured aerosol species should equal measured absorption.

A second data set consists of measured extinction using transmissometers and aerosol mass concentration measurements, including b_{abs}, by optical techniques in 18 monitoring sites in western national parks.

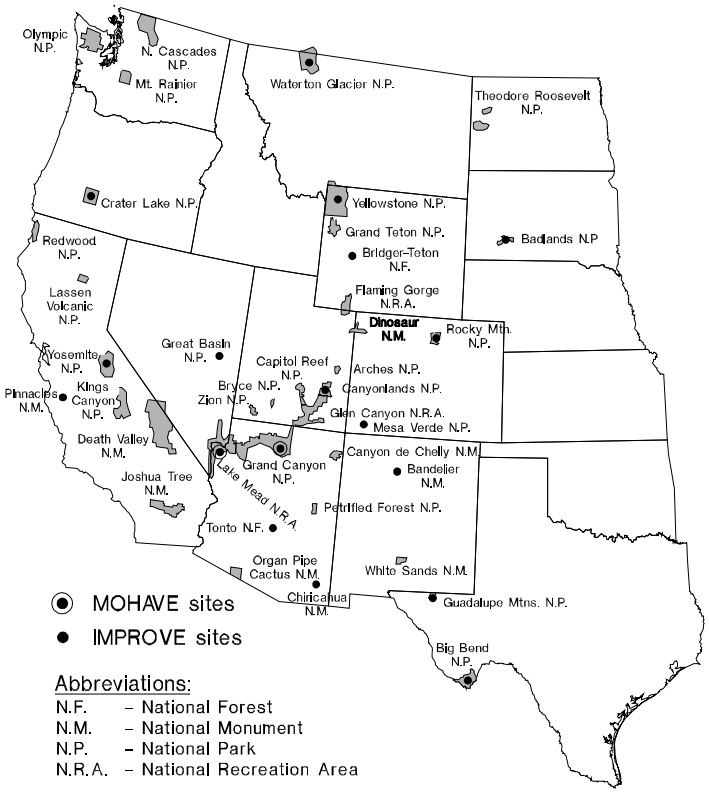

Figure 4.1 Map showing the location of monitoring sites and some of the larger national park units.

In many early visibility studies, comparisons were made between b_{scat}, as measured by nephelometry, and the various aerosol species to derive or validate scattering budgets, while extinction was estimated by summing absorption and scattering [Appel *et al.,* 1985; Ouimette *et al.,* 1981; Groblicki *et al.,* 1981; Macias *et al.,* 1981]. In many of these early studies the nephelometer sampling chamber was warmer than ambient temperatures and therefore underestimated scattering due to absorbed water at higher relative humidities. Furthermore, the absorption coefficient was not directly validated by independent methods.

More recent studies carried out in urban environments included estimates of extinction from teleradiometer techniques but utilized nephelometers, which heated the aerosol by about 4^oC [Dzubay and Clubb, 1981; Dzubay *et al.,* 1982; Lewis and Dzubay, 1986]. At 90% relative humidity (RH) a 1^oC difference between ambient and sampling chamber temperature will cause the sampling chamber relative humidity to reduce to about 84% RH. A 4^oC temperature difference translates into a chamber RH of 70%, which in turn results in a substantial underestimation of scattering from hygroscopic particles.

The most recent urban studies at Denver, Phoenix/Tucson, and Tucson [Watson *et al.,* 1988, 1989; Heisler *et al.,* 1980a,b; Watson *et al.,* 1990a,b; Heisler *et al.,* 1994] employed transmissometers to measure extinction [Dietrich *et al.,* 1989] ambient nephelometers to measure

scattering [Malm *et al.,* 1994] and integrating plate transmission measurements for absorption [Watson *et al.,* 1988, 1989]. These studies also included a full suite of aerosol measurements. For the most part, the sum of absorption and scattering equaled measured extinction within measurement uncertainty and measured absorption, and scattering could be predicted from aerosol measurements.

Only one study has explored the relationship between ambient measurements of b_{ext}, $b_{scat,}$ and b_{abs} in nonurban settings [White *et al.,* 1994]. They were able to show that the scattering and absorption as measured by optical techniques and the fraction of coarse mass scattering not captured by the nephelometer summed to extinction and were consistent with measurements of fine and coarse mass. They did not explore the relationship between measured absorption and estimates of absorption from aerosol concentrations.

4.1 Comparison of Reconstructed to Measured Fine Mass

Table 4.1 contains statistical summaries of the aerosol mass concentrations for the Meadview, AZ data set, along with the fraction that each aerosol species contributes to reconstructed fine mass, while Figure 4.2 is a scatter plot of reconstructed and measured fine mass. The error bars are calculated from reported measurement uncertainties. O1, O2, O3, O4, and OP have been multiplied by 1.4 to account for the assumed mass of oxygen and other elements in organic carbon.

Although water associated with hygroscopic aerosols was not explicitly measured, it is expected that a significant amount of water was retained on the filter when the filters were weighed. The filters were equilibrated in the laboratory at approximately 50% relative humidity, a value which is well above the relative humidity at which ammonium sulfate or other hygroscopic particles dry out [Tang *et al.,* 1981]. Therefore, retained water will cause scatter in the data points below, but not above, the 1:1 line because measured gravimetric mass includes some water, while reconstructed mass does not. Figure 4.2 clearly shows this trend.

Measured and reconstructed fine mass accounts for 33% and 31% of measured PM_{10} mass. Sulfates are the largest fraction of reconstructed fine mass at 56%. Soil and organic carbon are virtually tied for second at 19% and 16%, respectively, while light-absorbing carbon (LAC) is 3% and nitrates are 6%. It is worth noting that the sulfate mass fraction of fine mass is somewhat greater than reported by others for studies carried out in the same region: 42% at Zilnez Mesa by Macias *et al.* [1981], 40% at Glen Canyon by Sutherland and Bhardwaja [1990], and 40% at Meadview by Vasconcelos *et al.* [1994].

Table 4.2 is a similar summary of aerosol mass species concentrations for 14 western IMPROVE sites, while Figure 4.3 shows a scatter plot of reconstructed and measured fine mass. As with the Meadview data set there is more scatter below the 1:1 line suggesting that hygroscopic aerosols may have retained water during the weighing procedures. In the case of

Table 4.1 Summary statistics for aerosol mass concentrations for the summer Meadview data set. The number of valid data points is 97.

Variable	Mean (ìg/m^3)	Std Dev	Minimum (ìg/m^3)	Maximum (ìg/m^3)	Fraction of reconstructed fine mass
CM	9.60	3.84	3.29	18.14	--
FM	4.80	1.66	1.72	10.40	--
FM_{recon}	4.14	1.50	1.26	9.98	--
$(NH_4)_2SO_4$	2.31	0.95	0.93	6.68	0.56
NH_4NO_3	0.24	0.19	0.04	0.95	0.06
O1	0.02	0.11	-0.12	0.51	_0.01
O2	0.14	0.23	-0.26	1.27	0.03
O3	0.13	0.17	-0.19	0.59	0.03
O4	0.16	0.10	-0.03	0.62	0.04
OP	0.23	0.12	0.00	0.60	0.06
E1	0.04	0.05	0.00	0.26	0.01
E2	0.08	0.04	0.00	0.22	0.02
E3	0.01	0.02	-0.02	0.14	_0.01
SOIL	0.78	0.33	0.35	2.20	0.19
OMC	0.67	0.49	-0.25	2.59	0.16
LAC	0.13	0.08	0.00	0.42	0.03

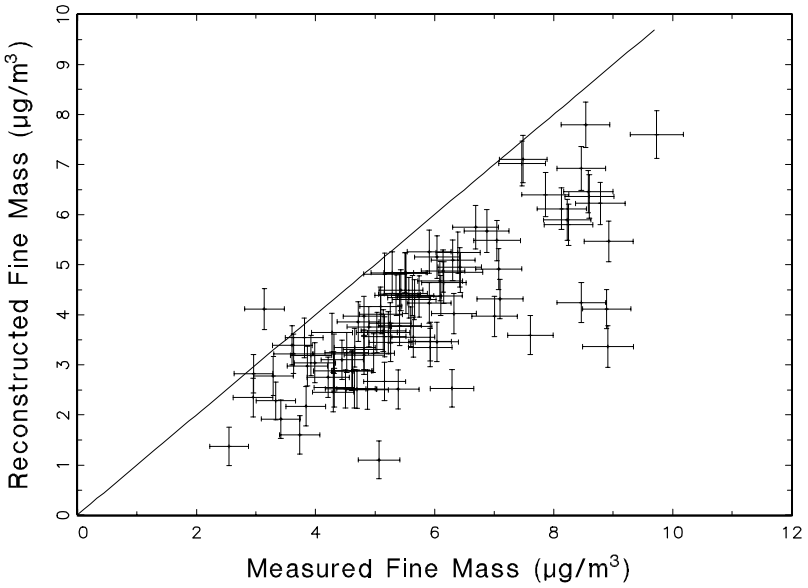

Figure 4.2 Scatter plot of measured and reconstructed fine mass for the summer Meadview data set. The error bars show the measurement uncertainty.

the IMPROVE sites, organic carbon is the largest fraction of fine mass at 41% with sulfate being second at 33%. Nitrates and LAC each contribute about 7% of the fine mass.

Table 4.2. Summary statistics for aerosol mass concentrations for the IMPROVE data set. The number of valid data points is 5108.

Variable	Mean (ìg/m^3)	Std Dev	Minimum (ìg/m^3)	Maximum (ìg/m^3)	Fraction of reconstructed fine mass
CM	4.81	4.48	0.00	72.43	--
FM	4.06	2.36	0.00	23.05	--
FM_{recon}	3.86	2.00	0.00	26.14	--
$(NH_4)_2SO_4$	1.26	0.87	0.00	9.45	0.33
NH_4NO_3	0.26	0.43	-0.06	10.15	0.07
O1	0.22	0.22	0.00	5.12	0.06
O2	0.32	0.22	0.00	4.11	0.08
O3	0.45	0.40	0.00	4.64	0.12
O4	0.28	0.23	0.00	3.06	0.07
OP	0.30	0.24	0.00	5.09	0.08
E1	0.11	0.15	0.00	2.42	0.03
E2	0.14	0.07	0.00	0.56	0.04
E3	0.03	0.03	0.00	1.37	0.01
SOIL	0.49	0.44	0.00	7.03	0.13
OMC	1.57	1.11	0.00	19.95	0.41
LAC	0.28	0.19	0.00	3.12	0.07

4.2 Extinction Components

The total extinction coefficient, $b_{ext,t}$, is the sum:

$$b_{ext,t} = b_{ext} + b_{ext,g}, where$$
$$b_{ext} = b_{scat} + b_{abs}, and \qquad (4.1)$$
$$b_{ext,g} = b_{scat,g} + b_{abs,g}.$$

b_{ext} and $b_{ext,g}$ are the extinctions due to particles and gases, respectively. b_{ext} is the sum of scattering, b_{scat}, and absorption, b_{abs}, by particles, while $b_{ext,g}$ is the sum of scattering, $b_{scat,g}$, and absorption, $b_{abs,g}$, by gases. All terms are wavelength dependent. Light scattering by gases in the atmosphere is described by the Rayleigh scattering theory [vandeHulst, 1981] and will be referred to as Rayleigh scattering. The only gas that is normally found in the atmosphere and absorbs light is nitrogen dioxide. In most instances, particle scattering and absorption are primarily responsible for visibility reduction [Trijonis and Pitchford, 1987].

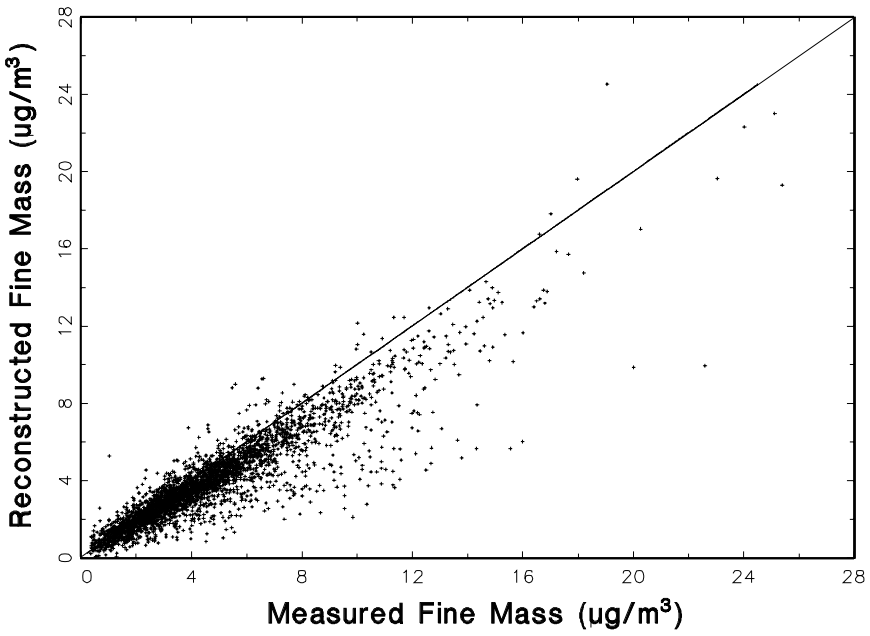

Figure 4.3 Scatter plot of measured and reconstructed fine mass for the IMPROVE data set.

Any particle in the atmosphere, whether it is externally or internally mixed, scatters and/or absorbs a specific amount of radiant energy and as such has a quantifiable mass extinction efficiency. White [1986] refers to this quantity as the specific extinction efficiency. Summing the extinction associated with each particle along some path must equal the total atmospheric extinction in that path. Therefore, a fraction of total extinction can be assigned to each particle type, and an extinction or scattering "budget" can be calculated.

Historically, researchers have invoked a number of assumptions concerning measured aerosol distributions. They have calculated or estimated specific mass scattering and absorption efficiencies, and used these to form estimates of extinction budgets. Because specific bulk aerosol species' concentrations are measured, the implicit assumption is one of externally mixed particles. However, under realistic assumptions concerning the microphysical properties of the particles the postulation of an external or internal mixture is not important to the estimation of specific mass extinction efficiencies. Ouimette and Flagan [1982] have shown that if an aerosol is mixed externally or if in an internally mixed aerosol the index of refraction is not a function of composition or size, and the aerosol density is independent of volume, then:

$$b_{ext} = \sum_i \alpha_i m_i \qquad (4.2)$$

where $\acute{a}_i$ is the specific mass scattering or absorption efficiency and m_i is the mass of the individual species. It should be pointed out, however, that as water is absorbed by hygroscopic particles the

index of refraction will change and that change will be dependent on the growth and mixture models that are assumed.

All routine aerosol monitoring programs and most special study visibility characterization programs were designed to measure aerosol species such as sulfates, nitrates, elements, and carbonaceous material [Heisler *et al*., 1980a; Malm *et al*., 1994; Tombach and Thurston, 1994; Watson *et al*., 1990a; and Macias *et al*., 1981]. They were not designed to determine whether these species were internally or externally mixed. Therefore, b_{ext} is usually apportioned by assigning specific mass extinction efficiencies to each species and calculating the total extinction using Equation (4.2).

A number of investigators have taken advantage of the form of Equation (4.2) to construct a multilinear regression model with b_{ext} as the dependent variable and the measured aerosol mass concentrations of species *I* as the independent variables. The regression coefficients are then interpreted as specific extinction to mass efficiencies [White and Roberts, 1977; Cass 1979; Groblicki *et al.,* 1981]. The use of multivariate regression models to apportion mass concentrations to scattering and absorption requires that the model meet a number of limiting assumptions, and should be used with caution. White [1986] discusses some of the issues associated with this problem.

Any apportionment of aerosol mass to extinction is only approximate. The assumptions required for extinction-mass relationships implied by Equation (4.2) probably are never exactly met. The appropriateness of any apportionment scheme can only be judged within the context of whether the model is physically "reasonable," and whether independent apportionment of mass to extinction is consistent with measurements of scattering and absorption.

The strategy used to examine extinction apportionment is to use Equation (4.2) to examine various relationships between measured scattering, extinction, and absorption, and between these variables and nominal dry particle extinction efficiencies that have been synthesized from a variety of estimates. Scattering associated with absorbed water is prorated among hygroscopic aerosol species. Regression analysis will be used to investigate the validity of assumptions utilized in the apportionment scheme.

4.2.1 Estimating Light Scattering

Because certain aerosols, such as sulfates and nitrates, have an affinity for water, their scattering characteristics change as a function of relative humidity (RH). Therefore, aerosol scattering of the so-called hygroscopic species as a function of relative humidity must be considered.

In general, the higher the RH the greater the scattering of soluble aerosols. The relationship between RH and scattering efficiency for ammonium sulfate aerosols with a mass mean diameter of 0.3 ìm and a geometric size distribution of 1.5 is shown in Figure 4.4. This function, referred to as *f*(RH), is:

$$f(RH) = b_{scat}(RH)/b_{scat}(0\%) \qquad (4.3)$$

where b_{scat}(0%) and b_{scat}(RH) are the dry and wet scattering, respectively. The aerosol growth was calculated following the scheme proposed by Tang [1981]. Ammonium sulfate and ammonium

nitrate mass are associated with this function.

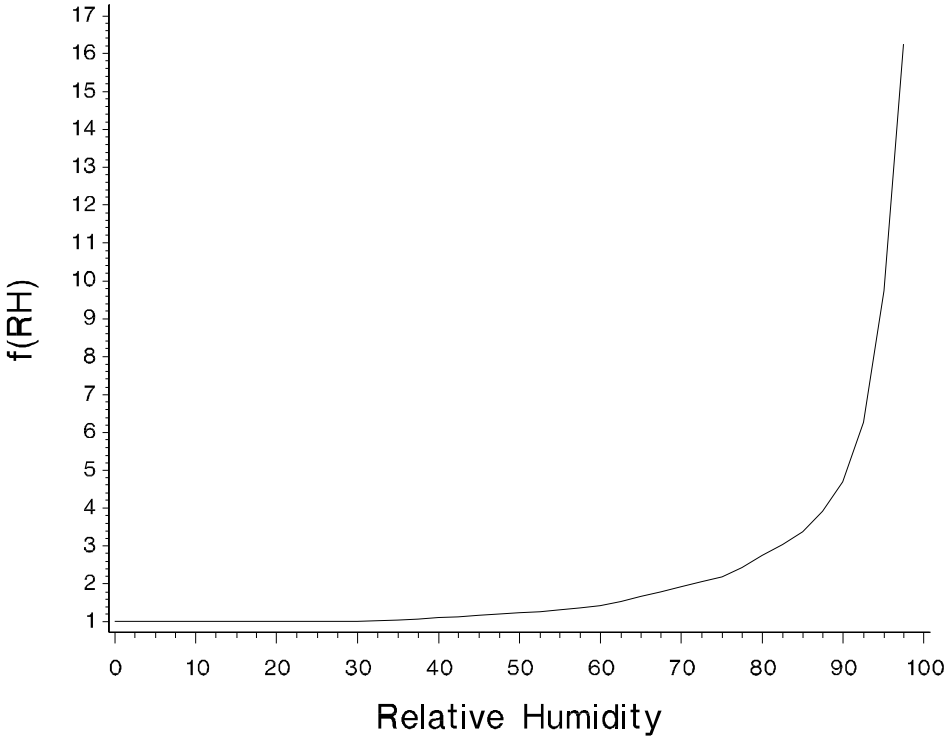

Figure 4.4 *f*(RH) for ammonium sulfate is plotted as a function of relative humidity.

Various functions for the hygroscopicity of organics have been proposed. Assumptions must not only be made about the solubility of organics but also on the fraction of organics that are soluble. White [1990] discusses this issue. Given the variety of organic species, it is possible that a geographic variation in organic species exists with large fractions of soluble species occurring in certain parts of the continent and much smaller fractions in other areas.

The following equation is used to estimate reconstructed particle scattering:

$$\begin{aligned} b_{scat} &= (3) f(RH)[SULFATE] \\ &+ (3) f(RH)[NITRATE] \\ &+ (3) f_{org}(RH)[OMC] \\ &+ (1)[SOIL] \\ &+ (0.6)[CM] \end{aligned} \qquad (4.4)$$

The brackets indicate the species concentration, 3 m^2/g is the dry scattering efficiency of sulfates, nitrates, and organic carbon, while 1 m^2/g and 0.6 m^2/g are the respective scattering efficiencies for soil and coarse mass. The efficiencies for fine soil and coarse mass are taken from a literature review by Trijonis and Pitchford [1987].

A dry scattering efficiency of 3 m^2/g is a nominal scattering efficiency based on a literature review by Trijonis *et al.* [1988, 1990] and a review by White [1990]. Trijonis' best estimate for sulfates and nitrates is 2.5 m^2/g with an error factor of 2, while for organics it is 3.75 m^2/g again with an error factor of 2. White [1990] took a somewhat different approach in that he reviewed 30 studies in which particle scattering and mass were measured. He then estimated a high and low scattering efficiency by using mass measurements to prorate the measured extinction. For sulfate the low estimate was arrived at by assuming that sulfate, nitrates, and organics scatter twice as efficiently as all other species, and for the high estimate he assumed that only sulfate was twice as efficient. His low and high sulfate mass scattering efficiencies for the rural west were 3.0 and 3.7 m^2/g, respectively. For organics, his low estimate assumes that organics and other nonsulfate species scatter half as efficiently as sulfates, and for the high estimate he assumes organics are three, and sulfates two times as efficient at scattering light as other species. His low and high estimates for organic mass scattering coefficients are 1.8 and 4.1 m^2/g. It is worth noting that an ammonium sulfate scattering efficiency of 3 m^2/g is also consistent with sulfur particle mass size distributions measured at Grand Canyon [Malm *et al.,* 1986].

The validity of using Equation (4.4) and the use of associated specific mass scattering efficiencies to estimate particle scattering from bulk measurements of aerosol species are explored in the next sections.

4.2.2 Estimating Aerosol Absorption

On channel A, b_{abs} is quantified directly by the LIPM analysis and is stated in units of 10^{-8} m^{-1}. It can also be estimated using Equation (4.2) in the form of:

$$b_{lac} = \alpha_{abs}[LAC] \qquad (4.5)$$

where á$_{abs}$ is the absorption efficiency of light-absorbing carbon. b_{lac} is used to represent particle absorption estimates derived from LAC mass concentrations. Horvath [1993] reviewed a number of studies where á$_{abs}$ for soot and black carbon were measured. He also reviewed a number of theoretical calculations of á$_{abs}$ where a variety of refractive indices and densities were assumed. Measured values of á$_{abs}$ range from a low of 3.8 to a high of 17 m^2/g, while theoretical calculations of á$_{abs}$ suggest a value of 8-12 m^2/g. The relationship between LAC and b_{abs} will be further explored in the following analysis.

4.3 Aerosol Scattering and Absorption

Table 4.3 presents the statistical summaries of the scattering or absorption associated with each variable for the summer Meadview data. The scattering associated with each species was calculated using the efficiencies presented in Equation (4.4) and an absorption efficiency for LAC of 10 m^2/g. Rb_{ext1} and Rb_{ext2} are reconstructed extinctions using b_{abs} and b_{lac}, respectively and Rb_{scat} is reconstructed scattering. Also presented in the table are summary statistics for measured b_{scat}, b_{ext}, ambient relative humidity (RH), and f(RH).

Table 4.3. Summary statistics for optical variables for the summer Meadview data set. The numbers reported are associated with the scattering, absorption, or extinction associated with each variable. Units on scattering, absorption, and extinction are in Mm^{-1}, while relative humidity is in percent and *f*(RH) factors have no units. Rb_{ext1} and Rb_{ext2} refer to reconstructed extinction using b_{lac} and b_{abs}, respectively and Rb_{scat} is reconstructed scattering. Units on scattering, absorption, and extinction are in Mm^{-1}, while relative humidity is in percent and *f*(RH) factors have no units. The number of valid data points is 82.

Variable	Mean (Mm^{-1})	Std Dev	Minimum (Mm^{-1})	Maximum (Mm^{-1})
b_{ext}	23.65	5.67	14.08	41.36
Rb_{ext1}	17.70	5.45	7.69	36.05
Rb_{ext2}	23.27	6.88	10.62	48.94
b_{scat}	12.44	5.22	4.33	36.83
Rb_{scat}	16.48	5.02	7.51	35.05
b_{abs}	6.80	2.07	3.11	14.93
b_{lac}	1.23	0.75	0.00	3.08
$(NH_4)_2SO_4$	7.23	3.15	3.01	20.03
NH_4NO_3	0.80	0.58	0.12	2.84
OC	1.88	1.24	-0.53	6.51
SOIL	0.80	0.34	0.35	2.20
CM	5.76	2.28	1.98	10.89
RH	25.79	13.25	6.08	61.92
f(RH)	1.06	0.12	1.00	1.63
$f(RH_c)$	1.05	0.11	1.00	1.60

The nephelometer chamber relative humidity is estimated from chamber temperature using:

$$RH_c = RH_a e^{\frac{5210.5(T_a - T_c)}{T_a T_c}} \qquad (4.6)$$

where RH_a, RH_c, T_a, and T_c are the ambient and chamber relative humidities and temperatures, respectively. From RH_c the $f(\mathrm{RH}_c)$ function inside the nephelometer can be estimated. It is also summarized in Table 4.3.

Because of the low relative humidities during the MOHAVE summer intensive, and because the "ambient" nephelometer exhibited minimal heating of the aerosol while in the sampling chamber, the $f(\mathrm{RH}_c)$ within the nephelometer was close to the ambient f(RH). The average f(RH) values for ambient and within the nephelometer were 1.06 and 1.05, while the maximum f(RH) values were 1.63 and 1.60, respectively. Because the f(RH) values were nearly the same, adjustments were not made to measured b_{scat} to account for chamber heating.

Figure 4.5 is a temporal plot of measured b_{ext}, b_{scat}, b_{abs}, ambient RH, and f(RH), while Figure 4.6 is a temporal plot of scattering associated with each aerosol species. Error bars were not included because of the unknown uncertainty in the prescribed efficiencies. The reported error on the b_{ext} and b_{scat} measurements are about 10%.

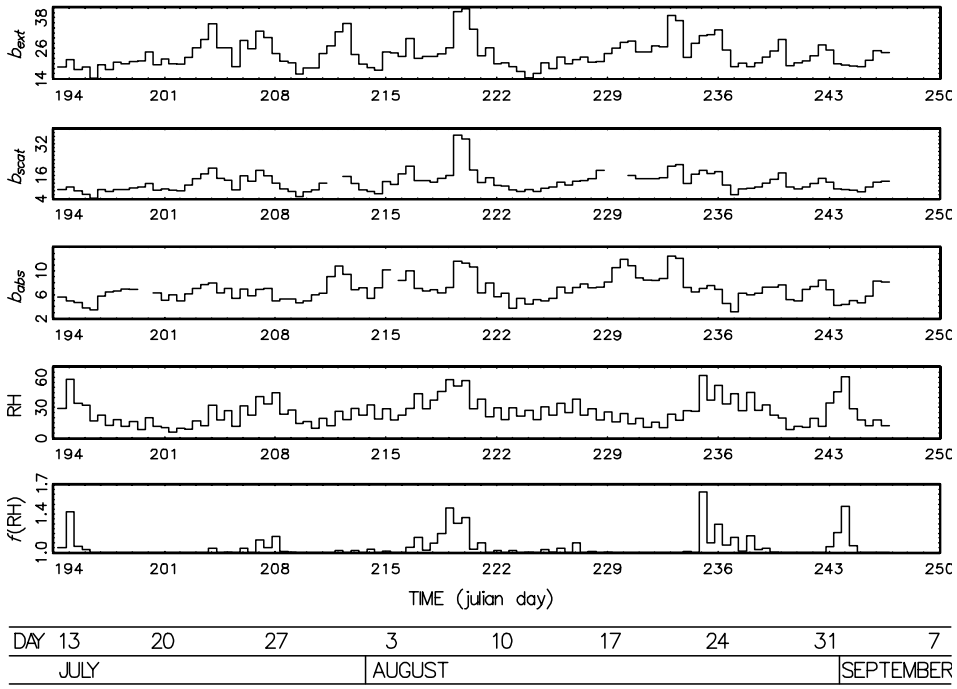

Figure 4.5 Temporal plot of measured b_{ext}, b_{scat}, b_{abs}, relative humidity, and f(RH) for the summer Meadview data set. Units on extinction, scattering, and absorption are Mm^{-1}, while relative humidity is in percent and f(RH) is unitless. Time is in Julian day, and for reference the month and day axis is also included.

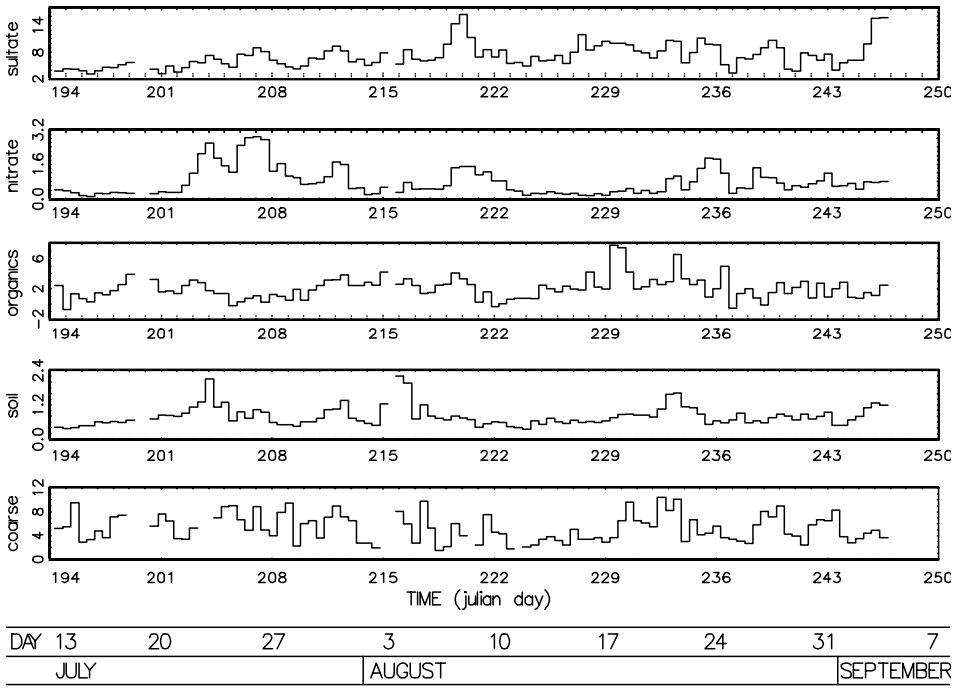

Figure 4.6 Temporal plot of estimated scattering associated with ammonium sulfate, ammonium nitrate, organics, fine soil, and coarse mass. Units are in Mm^{-1}.

Table 4.4 presents similar information for the IMPROVE data set. The scattering associated with each species was calculated using the efficiencies presented in Equation (4.4) and an absorption efficiency for LAC of 10 m^2/g. Of the 18 IMPROVE sites that have a transmissometer, nine sites were chosen to intercompare aerosol and b_{ext} measurements. They are Grand Canyon, Petrified Forest, Guadalupe Mountains, Yellowstone, Rocky Mountain, Glacier, Pinnacles, and Bandelier National Parks and Bridger Wilderness Area. At the other nine sites the transmissometer site path is directed over a slanted site path or over a canyon. Thus, the aerosol sampler and transmissometer are not sampling the same air masses.

The IMPROVE particle sampler collects samples for 24 hours, while the transmissometer and RH data is gathered on an hourly basis. Therefore, the transmissometer and RH data is averaged to 24 hours. There are about 5000 total data points consisting of 24-hr average transmissometer extinction, however, because of cloudy or foggy conditions not all 24-hr averages contain 24 data points. The analysis is restricted to those data points where there are at least 18 hourly readings for the transmissometer. With this restriction there remains 1642 valid readings.

Table 4.4 Summary statistics for optical variables for the IMPROVE data set. The numbers reported are associated with the scattering, absorption, or extinction associated with each variable. Units on scattering, absorption, and extinction are in Mm^{-1}, while relative humidity is in percent and *f*(RH) factors have no units. Rb_{ext1} and Rb_{ext2} refer to reconstructed extinction using b_{lac} and b_{abs}, respectively. The number of valid data points is 1642.

Variable	Mean (Mm^{-1})	Std Dev	Minimum (Mm^{-1})	Maximum (Mm^{-1})
b_{ext}	22.68	10.47	0.00	56.10
Rb_{ext1}	15.91	8.20	-0.32	59.70
Rb_{ext2}	20.41	10.02	0.92	67.97
b_{abs}	6.29	3.47	0.00	24.19
b_{lac}	1.79	1.71	-1.35	15.60
$(NH_4)_2SO_4$	4.76	3.39	0.18	28.52
NH_4NO_3	1.23	1.77	-0.24	23.09
OMC	3.87	2.33	-0.95	19.51
SOIL	0.71	0.62	0.02	4.35
CM	3.55	3.05	0.00	26.08
RH	46.67	15.30	7.79	87.17
f(RH)	1.45	0.44	1.00	3.91

4.4 Comparison of Reconstructed Extinction and Scattering

The Meadview data set offers a unique opportunity to examine the relationship among extinction, scattering and absorption directly without having to unduly rely on estimates of aerosol scattering from various species. Extinction, scattering, and absorption are all measured optically and thus allow for an independent assessment of the accuracy of these measurements. If the validity of these measurements can be established then scattering and absorption, as estimated from aerosol measurements, can be independently compared to each of these measures.

4.4.1 Extinction, Scattering, and Absorption Characteristics at Meadview

Extinction and scattering measurements are directly compared by using the following equation:

$$b_{ext} = b_{scat} + b_{abs} + CMS/2 \qquad (4.7)$$

where *CMS/2* is half the estimated total coarse mass scattering. Hasan and Lewis [1983] have carried out theoretical calculations to show that because of the forward angle truncation error in the nephelometer, it underestimates coarse mass scattering by about a factor of two. Furthermore, White *et al.*, [1994] were able to show from transmissometer derived total scattering and nephelometer measurements of fine and coarse particle scattering that the nephelometer underestimates scattering by particles greater than 2.5 ìm by about a factor of two.

Equation (4.7) consists of all measured optical variables except for CMS. Figure 4.7 is a scatter plot of the left and right side of Equation (4.7) along with the one-to-one line. Considering the uncertainty in estimated coarse mass scattering and the nephelometer response to coarse particles, the agreement is quite good. On the average, b_{ext} is only about 1 Mm^{-1} greater than $b_{scat}+b_{abs}+$ CMS/2. However, Figure 4.7 shows that for the main body of data points, b_{ext} is underestimated by about 2 Mm^{-1}, while the two largest extinctions are clearly overestimated.

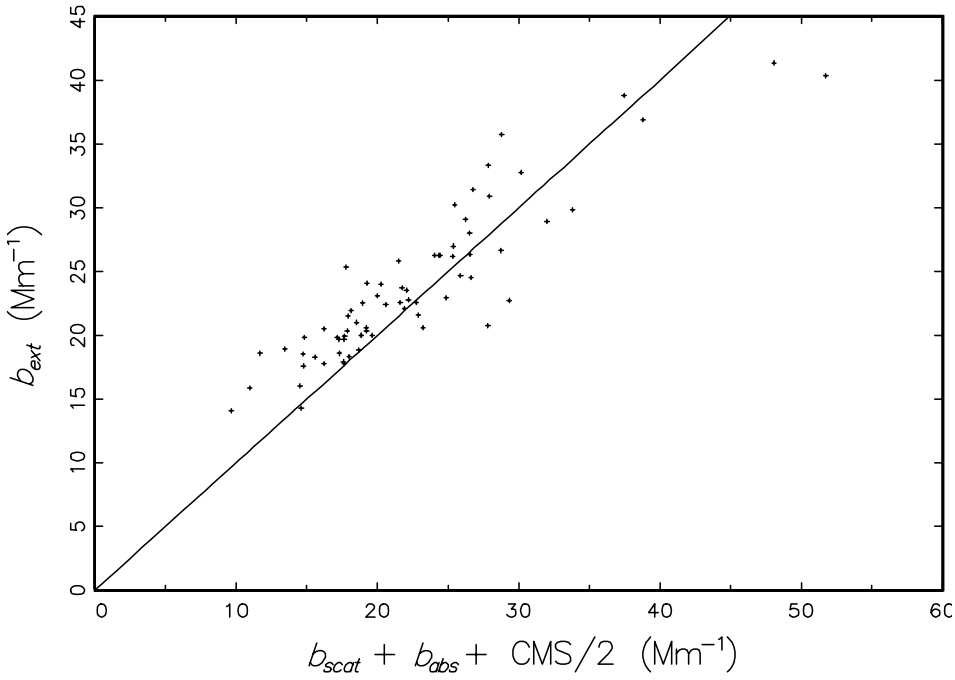

Figure 4.7 Reconstructed extinction using b_{scat}, b_{abs}, and coarse mass divided by 2 is plotted against measured extinction. Units are in Mm^{-1}.

In the above analysis b_{ext} was compared to reconstructed b_{ext} using the direct measurement of absorption, b_{abs}, by the laser integrated plate technique (LIPM) as opposed to using absorption estimates derived from LAC mass concentrations (b_{lac}). Figure 4.8 shows a scatter plot of reconstructed and measured extinction when b_{lac} is used as an estimate of absorption instead of b_{abs}. Using b_{lac}, which has been the traditional method of estimating b_{abs}, apparently yields an underestimation of extinction by about 7-8 Mm^{-1}. Examination of Table 4.4 shows that b_{abs} is 5.6 times larger than b_{lac}.

Using b_{abs} without any adjustments for reconstituting extinction gives a reasonable fit to measured extinction suggesting that b_{ext}, b_{scat}, and b_{abs} are accurate representations of ambient extinction, scattering, and absorption, while b_{lac} is not.

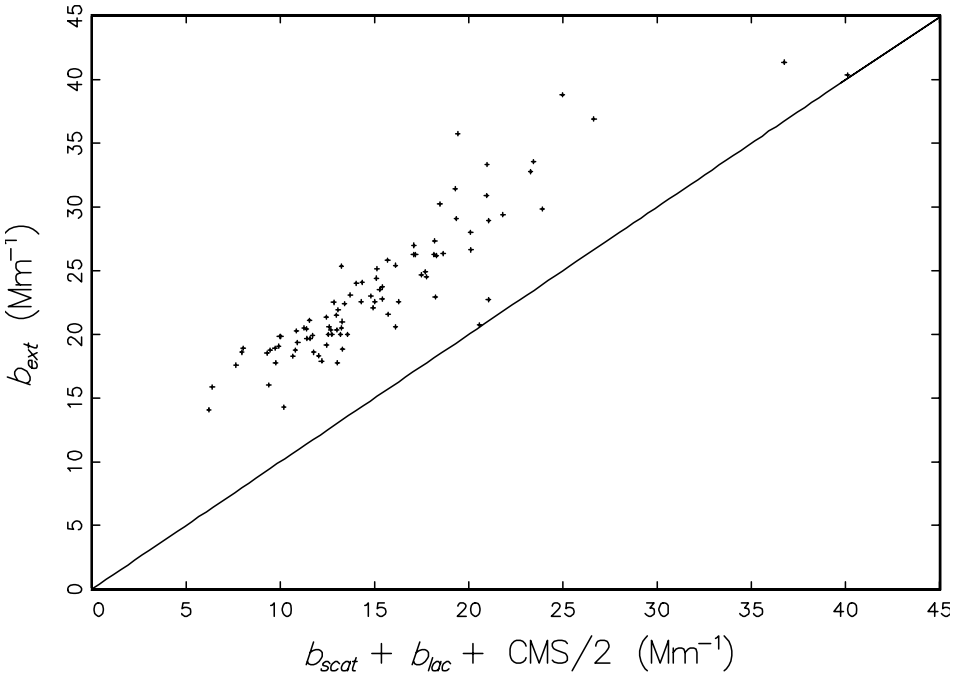

Figure 4.8 Reconstructed extinction using b_{scat}, b_{lac}, and coarse mass divided by 2 is plotted against measured extinction. Units are in Mm^{-1}.

4.4.2 Comparison of Estimated and Measured Scattering at Meadview

Figure 4.9 is a scatter plot of reconstructed and measured b_{scat} along with the 1:1 line for the summer Meadview data using CMS/2. Reconstructed scattering was calculated using Equation (4.4). The agreement is quite good. Most data points fall about the 1:1 line with the two highest measured values being about 7 Mm^{-1} greater than the 1:1 line. The close agreement between measured and reconstructed scattering gives some confidence that the aerosol species mass concentrations have been accurately measured and their associated scattering fairly represented.

4.4.3 Comparison of Estimated and Measured Extinction at Meadview and IMPROVE Sites

Figure 4.10 is a scatter plot of reconstructed and measured extinction using b_{abs}. Again, reconstructed b_{scat} was calculated using Equation (4.4). The agreement between reconstructed and measured extinction is quite good with reconstructed extinction being about 1 Mm^{-1} lower than measured extinction.

These results are consistent with the direct comparison between b_{ext}, b_{scat}, and b_{abs}. The real difference between the direct comparison of the optical variables is that the nephelometer scattering was corrected for underestimation of large particle scattering. In the reconstructions

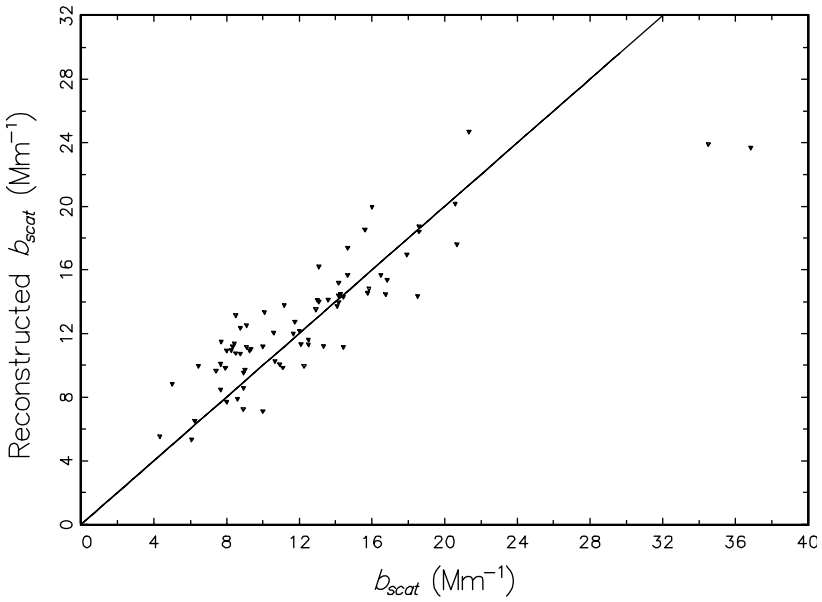

Figure 4.9 Reconstructed b_{scat} using the sum of estimated aerosol species scattering is plotted against measured b_{scat}. Units are in Mm^{-1}.

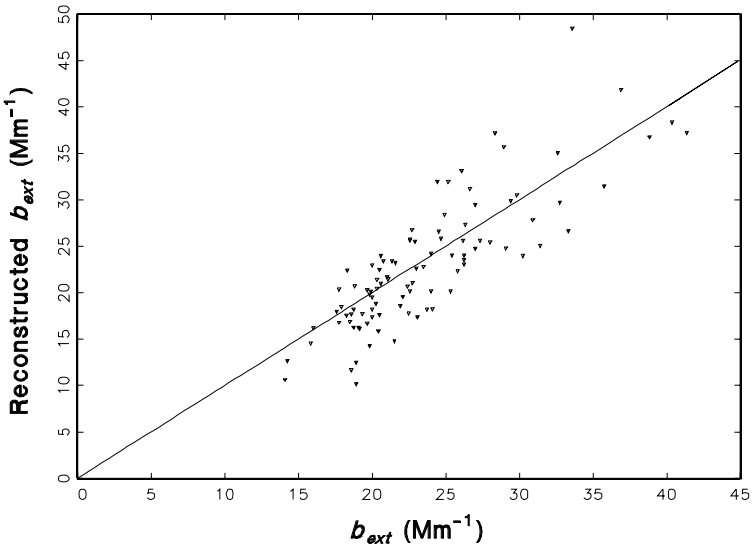

Figure 4.10 Reconstructed b_{ext} using the sum of estimated aerosol species scattering but with coarse mass scattering divided by 2 is plotted against measured b_{scat}. Units are in Mm^{-1}.

of extinction, this correction was not made because the transmissometer does not have a built-in underestimation of large particle scattering. In fact, the 0.6 m^2/g estimate of coarse particle scattering was derived from nephelometer measurements and it may be an underestimate of ambient coarse particle scattering and is certainly an underestimate of coarse particle absorption. Figure 4.10 suggests that the extinction in the 20-25 Mm^{-1} is somewhat underestimated, which may in part be due to an underestimation of coarse particle scattering and/or absorption.

The overriding issue, however, is the difference between b_{abs} and b_{lac}. The Meadview data set suggests that b_{abs} for the LIPM is a more accurate representation of absorption than b_{lac} as derived from LAC and that atmospheric absorption calculated using LAC may be a severe underestimate. The Meadview data set is small in that it covers about one month of time and is at only one location. The IMPROVE data set allows reconstructions of extinction using b_{abs} and b_{lac} to be compared with measured extinction over wide geographic regions and over a period of about four years.

Figures 4.11 and 4.12 are comparisons between reconstructed and measured extinctions using b_{lac} and b_{abs}, respectively, for the previously identified nine sites. As in the Meadview data set, reconstructed extinction is significantly lower than measured extinction when using b_{lac} and nearly the same when using b_{abs}. When using b_{lac}, reconstructed extinction is about 30% lower than measured extinction and about 10% lower when using b_{abs}.

For the reconstructed extinctions used in Figures 4.11 and 4.12 organics were not considered to be hygroscopic, and they were assumed to have the same dry mass scattering efficiency as sulfates. The hygroscopicity of organics was examined by assuming various fractions of organics being hygroscopic and assigning a variety of f(RH) curves to those fractions. Nonlinear growth curves caused the relationship between reconstructed and measured extinction to degrade as judged by the r^2 value associated with an ordinary least square (OLS) regression between the two variables.

The best fit between reconstructed and measured extinction, as judged by r^2 values, is achieved by increasing the dry mass scattering efficiency from 3 m^2/g to about 4 m^2/g. A 4 m^2/g dry mass scattering efficiency is consistent with the density of organics being lower than for sulfates. The resulting scatter plot between measured and reconstructed extinction is shown in Figure 4.13. The r^2= 0.63 with data points being nearly equally distributed above and below the 1:1 line. On the average, measured extinction is about 1 Mm^{-1} or 4% greater than reconstructed extinction. This difference is well within the uncertainties of the measurements.

The choice of scattering efficiencies used to match measured and reconstructed extinction are well within the constraints of known physical principles, however, they are by no means unique. The one outstanding feature is the need to use b_{abs} as derived from LIPM as opposed to b_{lac} to bring measured and reconstructed extinction into agreement. If b_{lac} is assumed to be the true atmospheric absorption any choice of growth functions, f(RH), and dry scattering efficiencies that force measured and reconstructed extinction to be equal are outside constraints imposed by known physical and chemical principles. Furthermore, the overall relationship between measured and reconstructed extinction is degraded as judged by r^2 values between the two quantities.

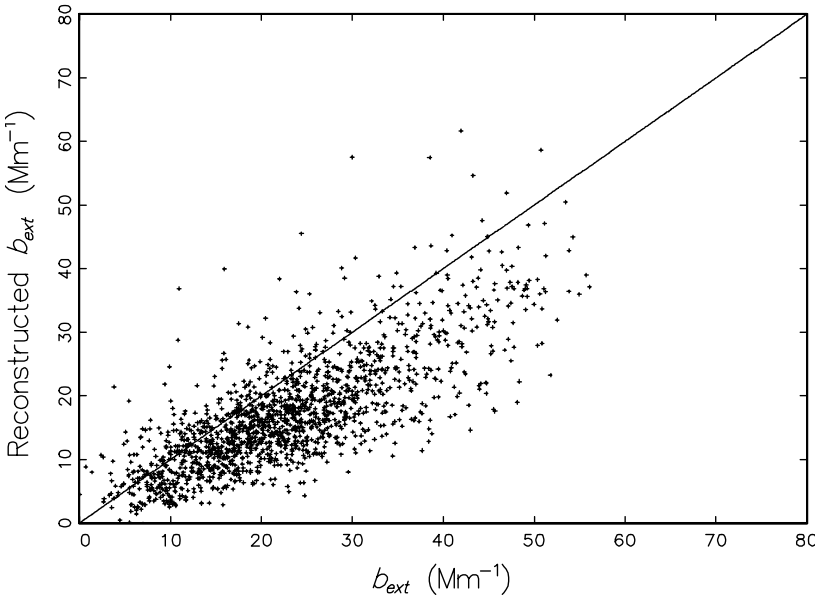

Figure 4.11 Reconstructed b_{ext} using b_{lac} and the sum of estimated aerosol scattering from the various aerosol species is plotted against measured b_{ext}. Units are in Mm^{-1}.

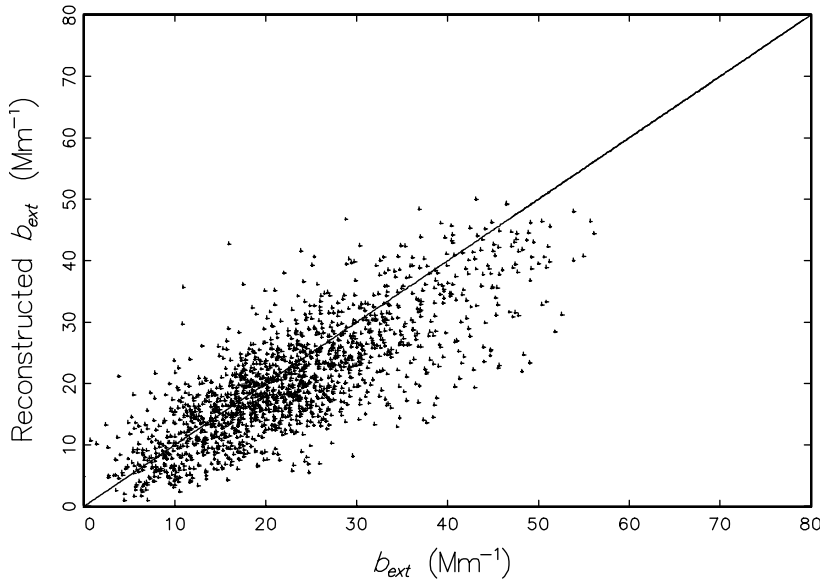

Figure 4.12 Reconstructed b_{ext} using b_{abs} and the sum of estimated aerosol scattering from the various aerosol species is plotted against measured b_{ext}. Units are in Mm^{-1}.

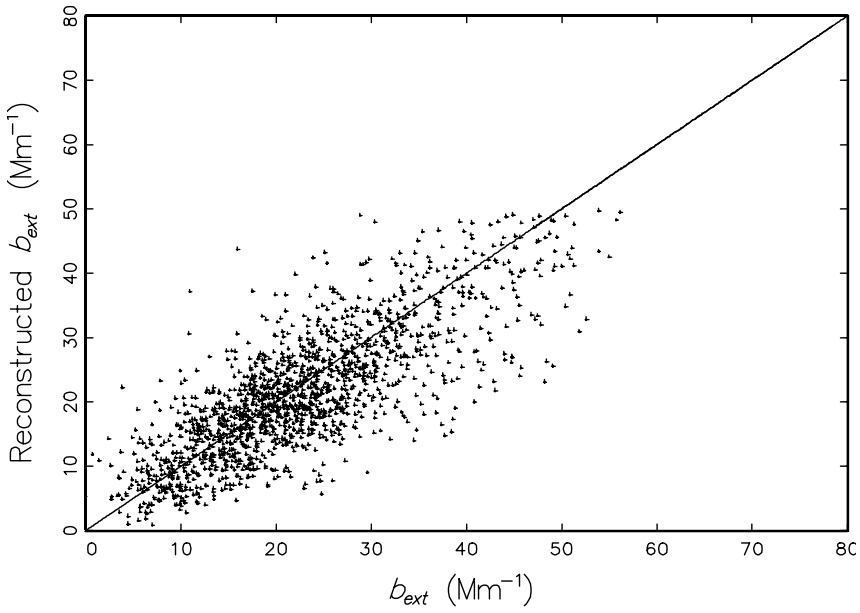

Figure 4.13 Reconstructed b_{ext} using b_{lac} and the sum of estimated aerosol scattering from the various aerosol species is plotted against measured b_{ext} for the IMPROVE data set. Units are in Mm^{-1}.

4.4.4 Regression Analysis

One can further examine the appropriateness of best estimates of scattering and absorption efficiencies using regressional techniques. Typically, the regression equation takes on the form of Equation (4.2) with either the extinction or scattering coefficient being the dependent variable and the aerosol species the independent variables. The regression coefficients are then interpreted as the scattering or absorption to mass efficiencies.

One problem with using regressional techniques is collinearity. One way to investigate the independence of variables is factor analysis. Table 4.5 presents a factor analysis using varimax rotation of the optical and aerosol scattering variables. b_{ext}, b_{abs}, b_{scat}, $SO_{4,scat}$, and $NO_{3,scat}$ are all loaded into the same factor, while organics (b_{lac}) and b_{abs} load into a second factor, and fine soil scattering ($soil_{scat}$) and scattering due to the sum of coarse mass and soil (CM_{scat}+$soil_{scat}$) load into a third factor. Therefore, for purposes of regression analysis sulfates and nitrates were combined into one variable, coarse mass and soil in a second, b_{abs} in a third, and organics in a fourth.

Table 4.5. Results of a factor analysis on various extinction, scattering, and absorption variables for the summer Meadview data set.

VARIABLE	FACTOR 1	FACTOR 2	FACTOR 3
b_{ext}	0.84663	0.25915	0.36179
b_{scat}	0.84947	0.33622	0.19281
$SO_{4,scat}$	0.84729	0.28517	-0.12735
$NO_{3,scat}$	0.67126	-0.42681	0.43896
OMC_{scat}	0.15304	0.84407	0.13199
$soil_{scat}$	0.24992	0.41696	0.62812
CM_{scat} + $soil_{scat}$	0.06930	0.09632	0.90461
LAC	0.25854	0.79690	0.14658
b_{abs}	0.63729	0.62277	0.24615
Variance explained by each factor			
	FACTOR 1	FACTOR 2	FACTOR 3
	3.170547	2.362169	1.689319

A three-step linear least squares regression was carried out on the following equations:

$$\begin{aligned} b_{ext} &= a_1(b_{scat}) + a_2(b_{abs}) + a_3(soilcms), \\ b_{ext} &= a_4(S4N3) + a_5(OMS) + a_6(b_{abs}) + a_7(soilcms), \text{and} \\ b_{scat} &= a_8(S4N3) + a_9(OMS) + a_{10}(soilcms). \end{aligned} \tag{4.8}$$

b_{scat}, b_{abs}, and b_{ext} are the measured variables, while *soilcms* is estimated soil plus coarse mass scattering. *S4N3* is estimated sulfate plus nitrate scattering, and *OMS* is estimated scattering attributed to organics. A three-step regression optimizes the coefficients for a best fit to all three equations simultaneously [Judge *et al.*, 1988, 1985].

Results of the regression is presented in Table 4.6. If the estimates of efficiencies are representative, the regression coefficients should equal one except for a_{10}, the *soilcms* coefficient associated with the nephelometer scattering, which should be closer to 0.5. (The nephelometer measures about ½ of the coarse mass scattering.) The coefficients are all surprisingly near one except for a_{10}, which is closer to the expected 0.5. The regression coefficients suggest that the estimates used for calculating scattering are correct, and more importantly b_{abs}, as opposed to b_{lac}, is the more accurate measure of absorption.

Table 4.6 Results of a three-step ordinary least square (OLS) regression with various optical variables as dependent and independent variables.

Dependent Variable	Independent Variable	Estimate	Std Error	t-value	r^2
b_{ext}	b_{scat}	0.93	0.21	4.4	0.65
	b_{abs}	1.06	0.42	2.5	
	soilcms	0.65	0.15	4.3	
b_{ext}	S4N3	0.94	0.16	5.9	0.56
	OMS	1.10	0.28	3.9	
	soilcms	1.01	0.16	6.3	
	b_{abs}	0.98	0.29	3.3	
b_{scat}	S4N3	0.96	0.09	11.3	0.66
	OMS	1.14	0.21	5.3	
	soilcms	0.36	0.10	3.6	

4.5 Attribution of Extinction to Aerosol Species

4.5.1 The Attribution Equation

Two unique data sets were used to explore the relationship between optical extinction, absorption, and scattering, and various aerosol species. The MOHAVE special study provided, at one monitoring site, independent optical measurements of b_{ext}, b_{scat}, and b_{abs}, and the various aerosol species. This data set provided for a variety of ways for exploring absorption and scattering efficiencies. A second data set, IMPROVE, provides for the first time, an opportunity to explore the relationship between measured extinction (as opposed to scattering) and aerosol species over the whole western United States. These are the first data sets where extinction was directly measured as opposed to estimated by summing b_{scat} and absorption as derived from "elemental" carbon measurements.

The most surprising outcome of the analysis relates to estimates of absorption. It has been known for some time that, at remote nonurban locations, b_{abs} as derived from the LIPM, was about twice the absorption as estimated from elemental carbon derived from thermal optical reflectance techniques (b_{lac}). Although there may be alternative interpretations, the most straightforward explanation of the relationships between b_{ext}, b_{scat}, b_{abs}, and b_{lac} is that b_{abs} is a more accurate predictor of absorption than b_{lac}.

Therefore, absorption estimates will be based on b_{abs}, while scattering apportionment will be based on Equation (4.4), but with the scattering efficiency for organic mass set equal to 4 m^2/g, and f_{org}(RH) set equal to one. The equation used for reconstructing extinction then becomes:

$$
\begin{aligned}
b_{ext} &= (3) f(RH)[SULFATE] \\
&+ (3) f(RH)[NITRATE] \\
&+ (4)[OMC] \\
&+ (1)[SOIL] \\
&+ (0.6)[CM] \\
&+ b_{abs}
\end{aligned}
\qquad (4.9)
$$

4.5.2 Estimating *f*(RH) from Average Relative Humidity

One remaining issue for the apportionment of scattering to hygroscopic aerosol species is the disparity between the instantaneous effects of relative humidity on scattering and the fact that aerosol samples are gathered on a 24-hour period. Light extinction and mass budgets involve averaging samples collected over a time interval. The extinction and mass budget represents the average contribution of each aerosol species to the average extinction or mass for the time interval. When soluble aerosols dominate the mass concentration, the distribution of RH over the interval becomes an issue. Failure to consider the distribution of RH can have significant effects on the average extinction attributed to the soluble aerosol.

Mass budgets, for a particular time interval, are calculated by finding the average concentrations of the individual species of fine mass, then dividing each by the sum of the averages. If the aerosol data can be time matched with RH data, then light extinction budgets can be calculated in a parallel fashion. Specifically, a light extinction for each species and each sample can be calculated. Thus, the average light extinction due to each species over the time interval can be estimated.

If collocated and time-matched RH data are not available, but reliable estimates of the average RH over the time interval are, then a first approximation of an average light extinction for a given species can be made. One initial approach would be to apply the RH correction factor associated with the average RH to estimate the average extinction due to a soluble species. However, it can be demonstrated that for sites where the average RH is high, this approach will seriously underestimate the average extinction of a soluble aerosol when the soluble aerosol concentration is independent of RH. This is due to the convex and highly nonlinear nature of the aerosol growth curves and the subsequent functions, f_T(RH). In the case of the *f*(RH) associated with Tang's growth curve, shown in Figure 4.4, Equation (4.9) holds

$$f_T\left(\overline{RH}\right) \leq \overline{f_T(RH)}. \qquad (4.10)$$

Moreover, if the distribution of soluble species concentrations are independent of RH, then

$$\overline{f_T(RH)c} \approx \overline{f_T(RH)}\,\overline{(c)} \qquad (4.11)$$

Equality would occur as a limiting value when the sample size increases without bound.

In this report, light extinction due to a soluble species at site *s* is derived using hourly RH values less than or equal to 98% and the equation is

$$b_{ext} = \beta F_{T,s} \bar{c}, \qquad (4.12)$$

where

$$F_{T,s} = \overline{f_T(RH_s)}. \qquad (4.13)$$

Using Equation (4.9), extinction budgets for a time interval may be calculated by replacing $f_T(RH_s)$ with $F_{T,s}$ and by using the average concentration of each species over the time interval as the mass concentration.

Using the data for the collocated sites, Figure 4.14 has the plot of Tang's RH dependent factor, as defined by Equation (4.12), versus annual average RH for the 39 IMPROVE sites with RH and light extinction measurements. A polynomial curve was fitted to the annual and seasonal data as defined by,

$$F = b_0 + b_2\left(100/\left(100 - \overline{RH}\right)\right)^2 + b_3\left(100/\left(100 - \overline{RH}\right)\right)^3 + b_4\left(100/\left(100 - \overline{RH}\right)\right)^4 \qquad (4.14)$$

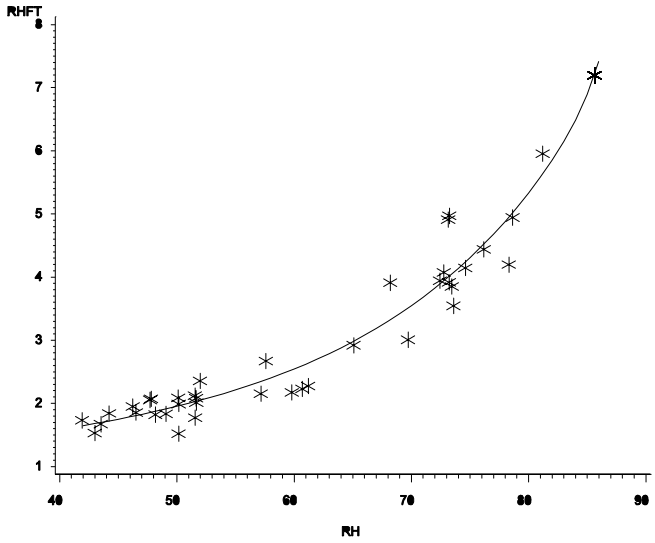

Figure 4.14Dependence on average site relative humidity of the relative humidity correction factor for sulfate ($F_{T,s}$) for the 39 IMPROVE sites with relative humidity measurements.

Table 4.7 shows the results of the regressions for Tang's weighted correction factors. The high r^2 values arise from the fact that the noise in the relationship is due primarily to differences in the RH distributions between sites. More explicitly, if two sites had the same average RH, their weighted factors would be the same if their RH distributions were identical.

Table 4.7 Parameters of the best-fit quadratic equation relating the relative humidity light extinction correction factors (F_T) to average site relative humidity ($F = b_0 + b_2(1/(1-rh))^2 + b_3(1/(1-rh))^3 + b_4(1/(1-rh))^4$).

Season	Intercept	T2	T3	T4	r^2
Spring	0.76	0.31	-0.004	-0.004	0.95
Summer	0.51	0.47	-0.081	0.004	0.95
Autumn	-0.03	0.83	-0.196	0.014	0.93
Winter	1.19	0.29	-0.033	0.001	0.87
ANNUAL	0.52	0.53	-0.095	0.006	0.94

In the IMPROVE monitoring network there are currently 55 sites operating that have fully complemented aerosol samplers (channels A-D); however, only those sites with a year or more of aerosol data are reported here. Of these sites, 39 have optical monitoring and hence RH data. Using the results of the regressions, annual and seasonal weighted factors were calculated for the additional sites by estimating their annual and seasonal average RH from weather service RH contour maps [NOAA, 1978] (Figure 4.15) or from alternate sources.

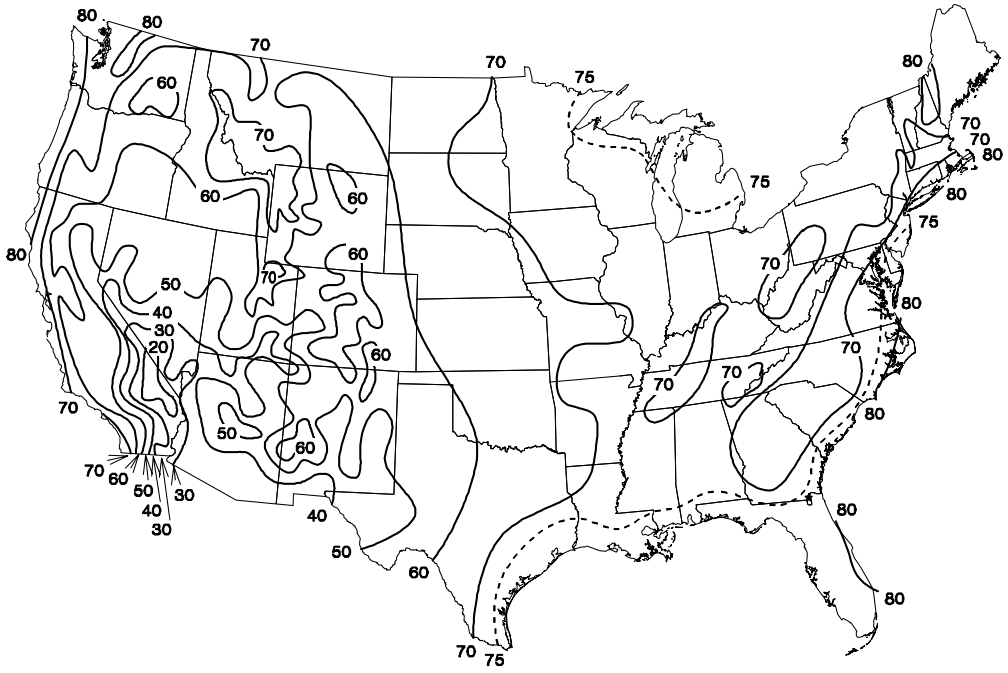

Figure 4.15 Spatial variation in annual average relative humidity [NOAA, 1978].

4.6 References

Appel, B.R., Y. Tokiwa, J. Hsu, L.E. Kothny, E. Hahn, and J.J. Wesolowski, Visibility as related to atmospheric aerosol constituents, *Atmos. Environ.*, **19**, 1525-1534, 1985.

Cass, G.R., On the relationship between sulfate air quality and visibility with examples in Los Angeles, *Atmos. Environ.*, **13**, 1069-1084, 1979.

Dietrich, D.L., J.D. Molenar, J.F. Faust, Transmissometer extinction measurements in an urban environment, In Visibility and Fine Particles, C.V. Mathai, Ed., AWMA, Pittsburgh, 1989.

Dzubay, T.G., and K.W. Clubb, Comparison of telephotometer measurements of extinction coefficients with scattering and absorption coefficients, *Atmos. Environ.*, **15**, 2617-2624, 1981.

Dzubay, T.G., R.K. Stevens, C.W. Lewis, D.H. Hern, W.J. Courtney, J.W. Tesch, and M.A. Mason, Visibility and aerosol composition in Houston, TX, *Environ. Sci. and Tech.*, **16**, 514-525, 1982.

Groblicki, P.J., G.T. Wolff, and R.J. Countess. Visibility-reducing species in the Denver "brown cloud"-I. Relationships between extinction and chemical composition, *Atmos. Environ.*, **15**, 2473-2484, 1981.

Hasan, H. and C.W. Lewis, Integrating nephelometer response corrections for bimodal size distributions, *Aerosol Sci. & Technol.*, **2**, 443-453, 1983.

Heisler, S.L., R.C. Henry, J.G. Watson, and G.M. Hidy, The 1978 Denver winter haze study volume II. ERT document #P-5417-1. Environmental Research and Technology, Inc., West Lake Village, CA, 1980a.

Heisler, S.L., R.C. Henry, and J.G. Watson, The source of the Denver haze in November and December 1978, Paper 80-58.6, presented at the 73rd Annual Meeting of the Air Pollution Control Association, Pittsburgh, PA, 1980b.

Heisler, S.L., I. Tombach, D. Fitz, J. Watson, and J. Chow, Tucson urban haze study, Final Report, Arizona Dept. Of Environmental Quality, Phoenix, AZ, Doc. #0493-005-804, 1994.

Horvath, H., Atmospheric light absorption - A review, *Atmos. Environ.*, **27**(A), 3, 293-317, 1993.

Judge, G.G., W.E. Griffiths, R.C. Hill, H. Lutkepohl, and T.C. Lee, "The theory and practice of econometrics", 2nd Edition, New York, John Wiley & Sons, 1985.

Judge, G.G., R.C. Hill, W.E. Griffiths, H. Lutkepohl, and T.C. Lee, "Introduction to the theory and practice of econometrics", 2nd Edition, New York, John Wiley & Sons, 1988.

Lewis, C.W., and T.G. Dzubay, Measurement of light absorption extinction in Denver, *Aerosol Sci.Tech.*, **5**, 325-336, 1986.

Macias, E.S., J.O. Zwicker, and W.H. White, Regional haze case studies in the southwestern United States II: source contributions, *Atmos. Environ.*, **15**, 1987-1997, 1981.

Malm, W.C., T.A. Cahill, K.A. Gebhart, and A. Waggoner, Optical characteristics of atmospheric sulfur at Grand Canyon, Arizona, In Visibility Protection, Research and Polisy Aspects, edited by P.S. Bhardwaja, pp. 418-433, 1986.

Malm, W.C., K.A. Gebhart, J.V. Molenar, T.A. Cahill, R.A. Eldred, and D. Huffman, Examining the relationship between atmospheric aerosols and light extinction at Mount Rainier and North Cascades National Parks, *Atmos. Environ.*, **28**, 347-360, 1994.

National Oceanic and Atmosperic Administration, Climatic Atlas of the United States, ESSA, Department of Commerce - 1968, Reprinted by NOAA, October, 1978.

Ouimette, J.R., and R.C. Flagan, The extinction coefficient of multicomponent aerosols, *Atmos. Environ.*, **16**, 2405-2419, 1982.

Ouimette, J.R., R.C. Flagan, and A.R. Kelso, Chemical species contributions to light scattering by aerosols at a remote arid site, In: E.S. Macias and P.K. Hopke, eds. Amer. Chem. Soc. Symposium, Series 167: Atmospheric Aerosol, 1981.

Sutherland, J.L. and P.S. Bhardwaja, Seasonal fine mass budgets through regression-application to the Glen Canyon SCENES data, In: Transactions of Visibility and Fine Particles, C.V. Mathai (ed), Air & Waste Management/EPA International Conference, Pittsburgh, PA, 207-212, 1990.

Tang, I.N., W.T. Wong, and H.R. Munkelwitz, The relative importance of atmospheric sulfates and nitrates in visibility reduction, *Atmos. Environ.*, **15**, 2463, 1981.

Tombach, I. and S.A. Thurston, The quality of the SCENES measurements: the roles of data quality goals and evolving technology, In *Proc. Aerosols and Atmospheric Optics: Radiative Balance and Visual Air Quality*, Air & Waste Management Association, Pittsburgh, PA, 1994.

Trijonis, J.C., and M. Pitchford, *Preliminary extinction budget results from the RESOLVE program*, edited by P.S. Bhardwaja, Visibility Protection Research and Policy Aspects, Air Pollution Control Association, Pittsburgh, Pa., 1987.

Trijonis, J.C. M. McGown, M. Pitchford, D. Blumenthal, P. Roberts, W. White, E. Macias, R. Weiss, A. Waggoner, J. Watson, J. Chow, and R. Flocchini, RESOLVE Project Final Report: Visibility Conditions and Causes of Visibility Degradation in the Mojave Desert of California, NWC TP #6869, Naval Weapons Center, China Lake, CA, 1988.

Trijonis, J.C., R. Charlson, R.B. Husar, W.C. Malm, M. Pitchford, and W. White, Visisbility: Existing and Historical Conditions-Causes and Effects. State of Science and State of Technology, Report No. 24. National Acid Precipitation Assessment Program, 1990.

vandeHulst, H.C., *Light scattering by small particles*, Dover Publications, New York, 1981.

Vasconcelos, L.A., E.S. Macias, and W. White, Aerosol composition as a function of haze and humidity levels in the southwestern U.S., *Atmos Environ* **28***(22)*, 3679-3691, 1994.

Watson, J.G., J.C. Chow, L.C. Pritchett, L.W. Richards, D.L. Dietrich, J. Molenar, J. Faust, S.R. Andersen, and C.S. Sloane, Comparison of three measures of extinction in Denver, CO, Paper #89-151.4, Presented at the Air Pollution Control Association Annual Meeting, 1989.

Watson, J.G., J.C. Chow, L.W. Richards, S.R. Anderson, J.E. Houck, and D.L. Dietrich, The 1987-88 metro Denver brown cloud air pollution study, Volume I: program plan. DRI document 8810.1F1, prepared for the Greater Denver Chamber of Commerce, Denver, CO, by Desert Research Institute, Reno, NV, 1988.

Watson, J.G., J.C. Chow, L.W. Richards, D.L. Haase, C. McDade, L.D. Dietrich, D. Moon, L. Chinkin, and C. Sloane, The 1989-90 Phoenix urban haze study. Volume I: program plan. DRI document 8931.1F, prepared for Arizona Department of Environmental Quality, Phoenix, AZ, by Desert Research Institute, Reno, NV, 1990a.

Watson, J.G., J.C. Chow, L.W. Richards, D.L. Haase, C. McDade, D.L. Dietrich, D. Moon, L. Chinkin, and C. Sloane, The 1989-90 pilot Tucson urban haze study. Volume I: program plan. DRI document 8931.3F, prepared for Arizona Department of Environmental Quality, Phoenix, AZ, by Desert Research Institute, Reno, NV, 1990b.

White, W.H., On the theoretical and empirical basis for apportioning extinction by aerosols: a critical review, *Atmos. Environ.*, **20**, 1659, 1986.

White, W.H., Contributions to light scattering, In: Acidic Deposition: State of Science and Technology Report 24, J. Trijonis (lead author), National Acid Precipitation Assessment Program, Washington, DC, pp85-102, 1990.

White, W.H. and P.T. Roberts, On the nature and origins of visibility-reducing aerosols in the Los Angeles air basin, *Atmos. Environ.* **11**, 803-812, 1977.

White, W.H., E.S. Macias, R.C. Ninger, and S. Schorran, Size-resolved measurement of light scattering by ambient particles in the southwestern U.S.A., *Atmos. Environ.*, **28***(50*), 909-921, 1994.